International Journal of Environmental Sciences
ISSN: 2229-7359
Vol. 11 No. 23s, 2025
https://theaspd.com/index.php

Modified Mofs-Coal Fly Ash Composites for Enhanced Efficiency in the Removal of Heavy Metal Ions from Aqueous Matrix

Swaroopa Chilkamarri[1], Venkatesham Kothabai[1], Vijayalaxmi Burri[1], Vijayatha Myadam[1], Venkataswamy Perala[1], Anjaneyulu Chatla[2], Sasikumar Boggala[2], Ramaswamy Kadari[3], Sreedhar Inkollu[4] Hari Padmasri Aytam[1]

[1]Department of Chemistry, University College of Science, Osmania University, Hyderabad 500 007, Telangana, India

[2]Catalysis and Fine Chemicals Department, CSIR - Indian Institute of Chemical Technology, Hyderabad-500 007, Telangana, India.

[3]ROHS laboratory, Centre for Materials for Electronics Technology, Cherlapally HCL (PO), Hyderabad - 500 051, Telangana, India

[4]Department of Chemical Engineering, Birla Institute of Technology and Science, Pilani, Hyderabad 500 078, Telangana, India.

***Corresponding author**

Email ID ahpadmasri@osmania.ac.in; ahpadmasri@gmail.com

Abstract: *Metal Organic Frameworks (MOFs) and Na-modified Coal Fly Ash (CFA) composites were prepared by solvo-hydrothermal method to enhance the toxic heavy metal ion removal from aqueous matrix as against their pristine forms. Al, Cu, Zr and Ga-BTC based MOFs were recognized as potential and efficient and adsorbents in the removal of Pb(II), Hg(II) and Cd(II) and among them Ga showed higher adsorption efficiency. Hence, Ga-amino terephthalic acid (Ga-ATP) MOF is synthesized and tested for these metal ions removal. Further, MOF-CFA composites and Ga-ATP MOF were well characterized by XRD, SEM-EDX, FT-IR, Raman, UV-DRS, N_2 sorption and XPS. The metal ion removal was estimated by ICPOES and SEM-EDX analyses. All the four BTC MOFs composites with CFA have shown enhanced adsorption for the heavy metal ion removal and among them Ga BTC MOF-CFA composite showed exceptionally high adsorption capacity for Pb(II) ions of about 1983 mg/g from aqueous matrix. Ga-ATP MOF also exhibited high removal efficiency for Pb(II) ions of 1560 mg/g. Ga BTC MOF-CFA composite was found to be stable and regenerable for 5 runs of adsorption cycles.*

Keywords: *BTC, MOF, CFA, ATP, heavy metal ion, adsorption, ICP-OES, SEM-EDX*

1. INTRODUCTION

Metal Organic Frameworks (MOFs) are considered as wonder materials due to their unique properties that makes them ideal materials for numerous applications. They are also known as coordination polymers (PCPs) as they form networking structures through coordination bonds and supramolecular interactions with metal ions and organic linkers that are multidentate in nature [1]. The voids in the structures act as pores mostly being microporous with some mesopores also formed in the structure. This spread-out structure generates a high surface area and porous material which may be used as an adsorbent in environmental remediation, gas adsorption and storage, as catalysts in several organic transformation reactions, as bio/chemical sensors, magnetic materials, drug delivery systems, find applications in rechargeable batteries, supercapacitors, in tribolic and piezoelectric nanogenerators [2-8]. They are highly tunable microcrystalline, microporous, high surface area materials with unique morphology, controllable size, high stability and possess multifunctionalities owing to which they find diverse applications in various fields [9-12]. One of the important applications among them is removal of toxic heavy metal ions from water by adsorption utilizing the high surface area, porosity and congruence to functionalization and chelating properties of MOFs.

Heavy metal ions are toxic even if present in low concentrations in water, soil or air contaminating the environment that has detrimental effect not only on the flora and fauna but also on humans directly or indirectly [13-16]. The heavy ions are used in metallurgy, leather tanning, electroplating, steel fabrication, chemical and textile industries. Several physico-chemical techniques such as ion-exchange, ultrafiltration, precipitation, electrochemical and adsorption techniques are explored in the removal of these toxic metal ions [17]. Chemical adsorption using small amounts of adsorbents that are reusable is the best method being low-cost, selective and effective in the removal of toxic metal ions from water [18]. Adsorbents such

as carbons, clays, nanohybrids, silica- based materials etc., have been extensively explored in this regard [19-21]. Coal fly ash is an adsorbent that exhibited good adsorption capacity for the removal of heavy metal ions from water [22-24]. Fly ash is obtained in huge amounts in the mining industry, and its disposal is serious issue hence, its utilization in the remediation of heavy metal ions serves dual purposes. Also fly ash is a cheaper material and is abundantly available in nature. However, fly ash needs to be treated before use to remove unburnt coal and other impurities. Several MOFs viz., Mn-MOF [25], ZIF-90, DUT-67 (Zr)[26], UiO_2-66-NH_2 [27], Zn-MOF [28], Cu-MOF [29] etc., were reported for the effective removal of various heavy metal ions and also MOF composites and nanohybrids were studied for the remediation of toxic heavy metal ions in water [30, 31]. Our previous study on the removal of heavy metal ions over various BTC linked MOFs showed good adsorption efficiency of these materials [32]. A composite of the Na modified CFA with ZIF material is reported to enhance the adsorption of CO_2 [33]. To further enhance the adsorption capacity of BTC MOFs, their composites with Na modified CFA were prepared by in-situ solvo-hydrothermal method and explored for the removal of toxic heavy metal ions from water. Yet another modification of Ga BTC MOF which displayed the highest adsorption efficiency among the four different BTC linkaged MOFs studied previously was done by changing the organic linker to from benzene tricarboxylic acid to amino terephthalic acid with an intention to incorporate a 'N' containing ligand that can enhance the adsorption capacity of the MOF obtained [34]. The present work is focused on the study of removal of toxic heavy metal ions over MOF-CFA composites.

EXPERIMENTAL METHODS

Materials used

Nitrates of Aluminium, Copper and Gallium; $ZrCl_4$; trimesic acid; 2-amino terephthalic acid; coal fly ash; NaOH; $NaAlO_2$; N, N-DMF; methanol; acetone; aqueous solutions of Pb (II); Hg (II) and Cd (II).

Preparation of MOF-CFA composites

Composites of MOFs with Na modified coal fly ash were prepared by in-situ solvo-hydrothermal method where CFA is taken in 70% with 30% MOF in the resultant composite material. Four different composites with Ga BTC, Al BTC, Zr BTC and Cu BTC MOFs synthesized with the addition of calculated amount of CFA in their respective metal precursor solution following the same procedure used for the synthesis of the four different MOFs reported in our previous work [32]. Na modified coal fly ash was obtained by treating coal fly ash with sodium precursor as reported by Aniruddha et al. [33]. The Ga BTC MOF-CFA composites of varying compositions of MOF and CFA ranging from 0.1, 0.2 and 0.4 of Ga BTC and rest in the composites being CFA material were synthesized similarly as mentioned above.

Ga - amino terephthalic acid (ATP) MOF was prepared with gallium nitrate as the metal precursor (1 mmol)(0.4172 g) and following the similar procedure used for Ga BTC MOF [32] replacing BTC by 2-amino terephthalic acid(1.2 mmol) (0.21738 g) each in 12 mL DMF that were magnetically stirred and heated hydrothermally for 24 h at 100 °C. The mixture was cooled to the room temperature and centrifuged (8000 rpm, 5 min) to obtain white precipitate followed by washing with DMF for at least three times.

Characterization of the MOF-CFA composites

All the MOF-CFA composites and Ga-ATP MOF synthesized were characterized by XRD using a benchtop Rigaku miniplex diffractometer recorded using CuK_α radiation which is Ni filtered with 2theta in the range of 5-80° and the SEM-EDX analyses of the samples were done on a JEOL, JSM—6390LV and Oxford XMX N instrument. N_2 sorption studies of the samples were carried out at -186 °C using a Micromeritics ASAP 2010 instrument for evaluating BET isotherms and determining the pore characteristics of the adsorbents in this study. The thermograms in the TGA analysis were obtained over a Perkin Elmer STA 6000 instrument from room temperature to 800 °C heated at a rate of 20 °C/min. A JASCO V650 UV–Visible spectrophotometer is used to record the UV-visible spectra of the samples and a Thermo-Fisher Scientific instrument was used for FT-IR spectra of samples recorded from 400-4000 cm^{-1}. Raman spectra were recorded on HORIBA JOBIN YVON HR800, Japan with a 633 nm He-Ne LASER source. The surface analysis of the samples was done using a KRATOS-AXIS 165 XPS instrument with MgK_α radiation as the source of x-rays.

Adsorption studies in the heavy metal ion removal

A definite and required amount of MOF/MOF-CFA composite was taken in about 50 mL of variable concentrations of aqueous solutions of heavy metal ions and stirred at ambient temperature. From time to time the small aliquots of solutions after centrifugation were collected and subjected to ICPOES

analysis to determine the amounts of remaining metal ions in the solutions and the adsorbent after filtration to SEM-EDX to confirm the adsorbed metal ion compositions over the adsorbents. The % heavy metal ion removal efficiency from ICPOES analysis was done by using the formula = $\frac{C_0 - C_t}{C_0}$ x 100 where C_0 and C_t are the initial concentration prior to adsorption and concentration of the left out heavy metal ions at time 't' after adsorption respectively.

RESULTS AND DISCUSSION

X-ray Diffractograms

The XRD pattern of Ga MOF-CFA composite in the figure 1 above displayed broader peaks as compared to the pristine Ga BTC MOF [32]. 2 theta values at 13.97°, 24.31°, 31.62°, 34.59°, 42.75°, 51.93°, 58.14° and 69.44° indicate the diffraction lines corresponding to the crystalline Na modified coal fly ash (CFA). The d lines of the MOF and those of CFA seems to be merged in the broad peaks obtained. While the peaks in Al and Zr MOFs were dominated by the CFA characteristic lines which is the major component of the composite material. However, the additional peaks observed in the range of 30-40 and 50-60 deg. indicate the presence of MOFs in the composites. Cu-BTC MOF composite with CFA retained MOF characteristic peaks to mostly along with the CFA peaks indicating the crystallinity of this MOF composite is higher in comparison to the rest of the BTC MOF composites. Ga-ATP displayed diffraction lines at 8.3°, 9.61°, 14.43°, 16.69°, 17.38°, 19.29° and 26.97° that are characteristic of the amino terephthalic acid linked Ga MOF [35]. The simulated pattern match with that in this report have been suggested to have retained the Kegome topology.

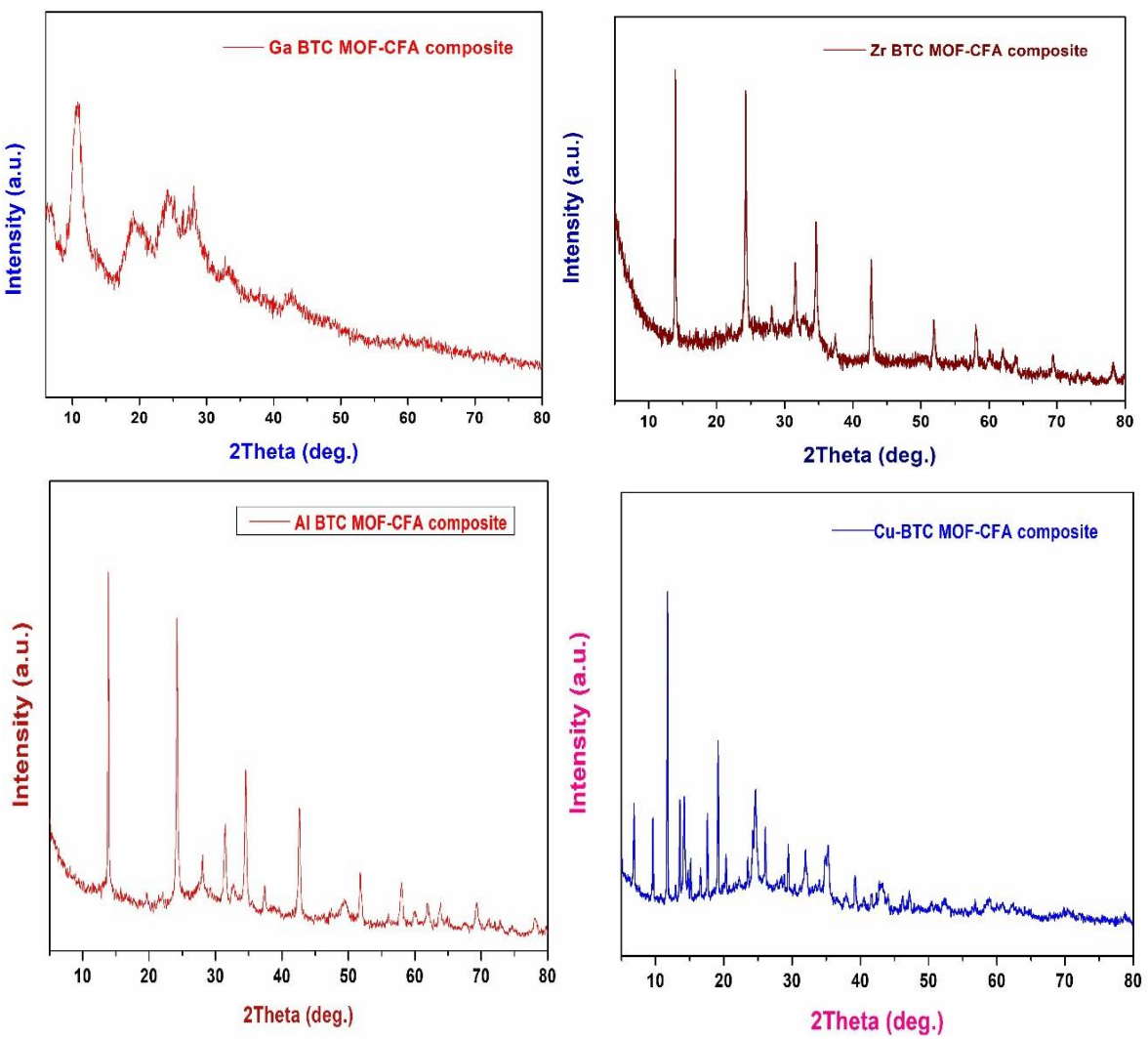

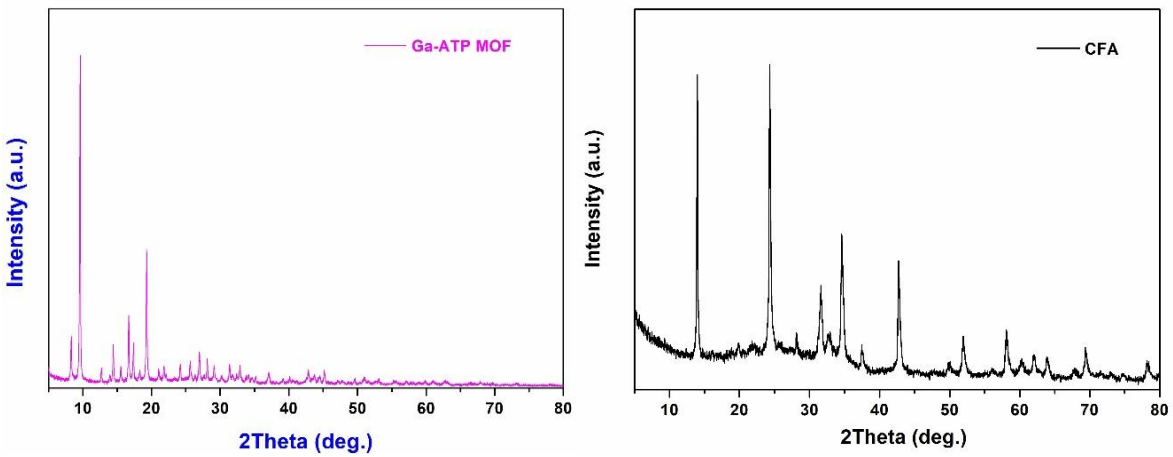

Figure 1: X-ray diffraction patterns of the CFA, Ga, Zr, Al & Cu BTC MOF-CFA composites and Ga-ATP MOF

Table-1: Structural characteristics of MOFs

Adsorbent	BET-SA (m^2g^{-1})	Average Pore radius (nm)	Pore volume (cc/g)
Cu-BTC-CFA	441	0.160	0.1000
Ga-BTC-CFA	408	0.321	0.0157
Al-BTC -CFA	528	0.260	0.0677
Zr-BTC -CFA	362	0.250	0.1100
Ga-ATP-MOF	1023	0.155	0.3300

Surface area and porosity characteristics

Figure 2 below depicts the N_2 adsorption isotherms of the MOF-CFA composites which are quite similar to the MOF materials falling in the type I kind indicating the presence of micropores retained even when large portion of the composite is dominated by CFA. However, the surface area and porosity dropped significantly in comparison to their pristine forms as the surface area of CFA is much lower compared to the MOFs. The porosity of the materials also had small amount of mesopores along with the micropores. The CFA composite with ZIF-8 prepared by in-situ method was shown to exhibit better surface are of the resultant composite as compared to a physical mixture and an impregnated one [33]. Hence, in-situ method was chosen in the present study as well for synthesizing MOF composites with CFA. Table 1 shows the sorption characteristics of the composites and Ga-ATP MOF which displayed high surface area representative of a MOF.

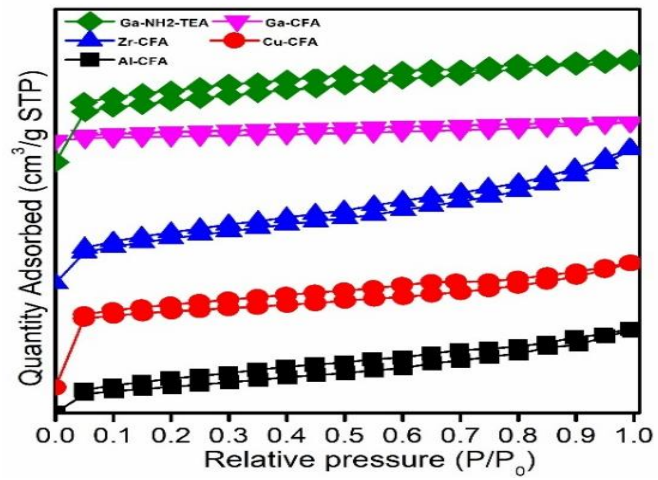

Figure 2: N_2 adsorption-desorption isotherms of MOF-CFA composites and Ga-ATP MOF

International Journal of Environmental Sciences
ISSN: 2229-7359
Vol. 11 No. 23s, 2025
https://theaspd.com/index.php

Morphological studies

The SEM micrographs presented in the figure 3 indicate a mixed morphology of the materials, presence of CFA changed the MOF morphology which could be seen in the reduction of crystallite size observed from XRD studies (broadening of peaks) as well.

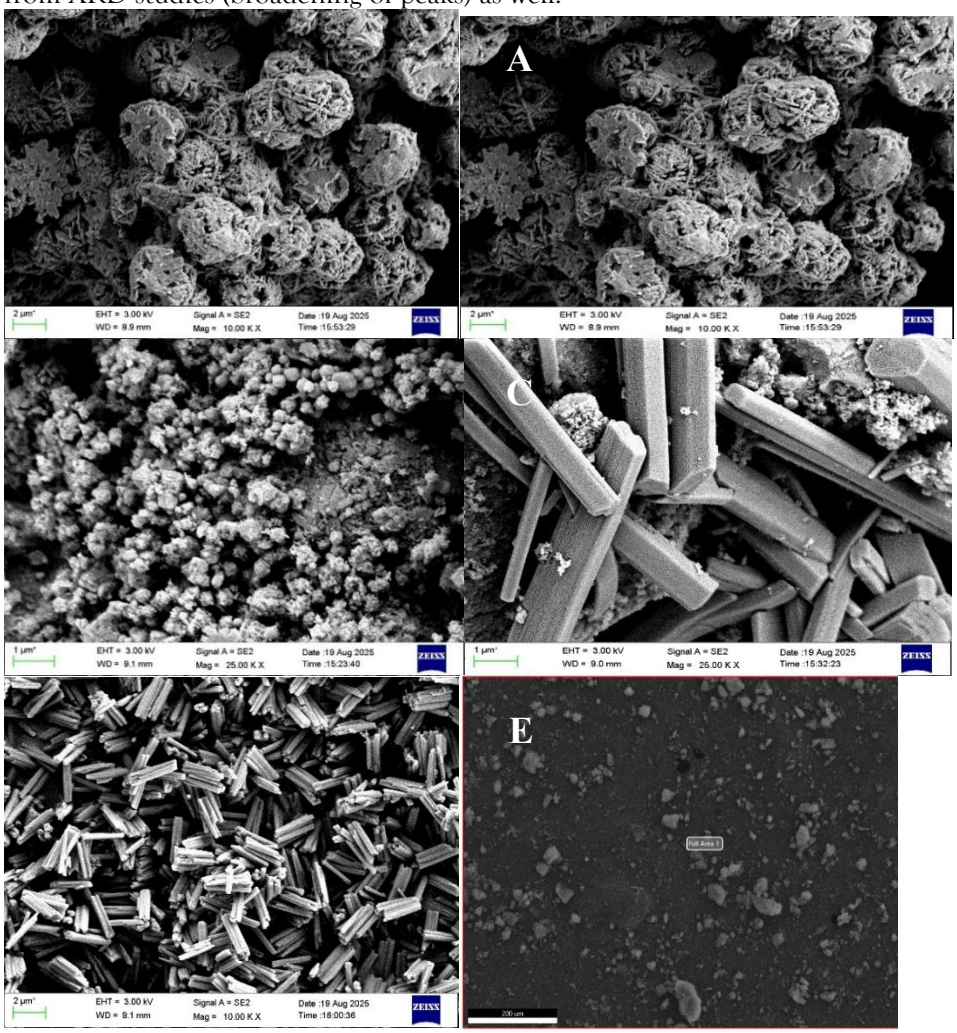

Figure 3: SEM micrographs of composites of CFA with MOFs A) Al-BTC B) Zr-BTC C) Cu-BTC D) Ga-BTC and E) Ga-ATP MOF; F) CFA

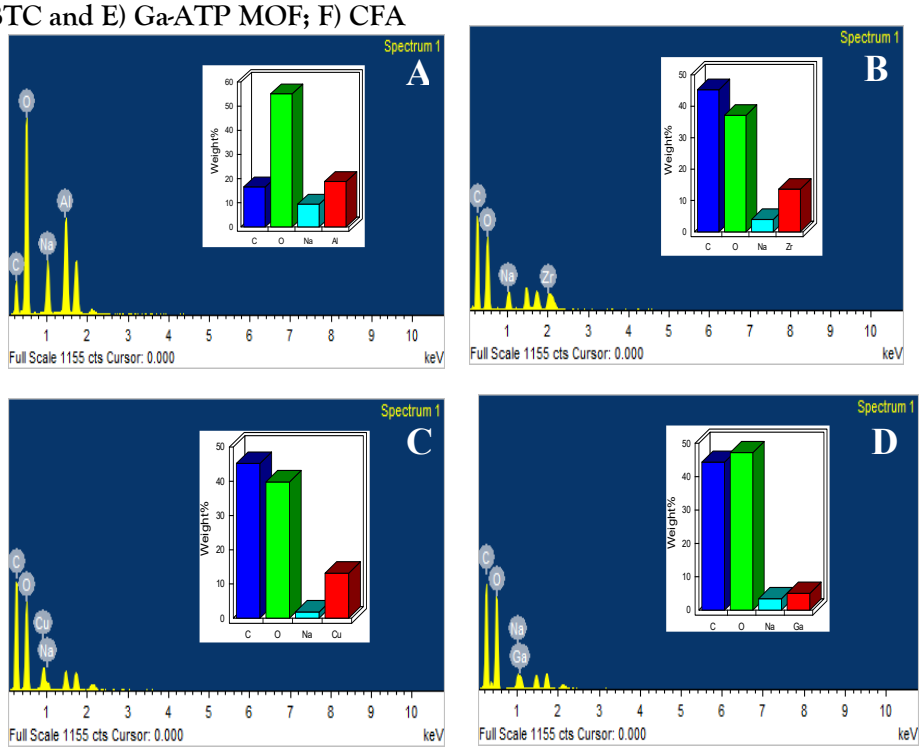

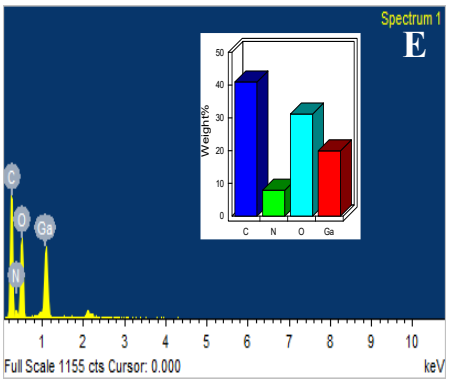

Figure 4: EDX spectra of composites of CFA with MOFs A) Al-CFA B) Zr-CFA C) Cu-CFA D) Ga-CFA and E) Ga-ATP MOF

The pure form of BTC MOFs were of cubo-octahedral/polyhedral shaped particles in the range of 50-100 nm. The morphology of the CFA composites of Al BTC, Zr BTC show that the insertion of CFA material into the cubo-octahedral/polyhedral particles resulting in rope bundle-like morphology with MOF entwining the CFA. The particles were found to be uniformly the distributed. The morphology of Cu BTC MOF-CFA composite retained the cubo-octahedral shape but these polyhedrons are much smaller than their pristine MOF and presence of CFA could be noticed dispersed in between the MOF particles. Ga MOF-CFA composite showed a different morphology of hexagonal rods as against the dodecahedral morphology of the Ga-BTC MOF. Ga-ATP MOF also showed smaller, well dispersed and uniform particles of hexagonal rod like morphology. The EDX spectra displayed the elemental compositions of all the above composites and Ga ATP MOF is right proportions. The inset figures in figure 4 of the EDX spectra clearly shows the % composition of all the elements present in the materials under study.

FT-IR results

Figure 5 below depicts the FT-IR spectra of the CFA, MOF-CFA composites and Ga-ATP MOF. It clearly shows that all the composites displayed the characteristics peaks of CFA as it is the major component of the composites. CFA spectra indicated the presence of Al-O, Si-O, Si-O-Si/Al-O-Si vibrational modes around 465, 670 and 970 cm^{-1} respectively [36]. While the vibrations of the O-H bond with the water molecules associated with CFA were found at 1653 cm^{-1} with 1400 cm^{-1}. And additional peaks observed correspond to the MOFs i.e., the vibrational modes of the BTC linker and metal-carboxylate bonds [32]. Ga-ATP MOF displayed bands at 1626 and 1258 cm^{-1} corresponding to N-H bending and C-N stretching modes respectively along with two peaks attributed to the symmetric and asymmetric stretching vibrations of the aromatic amino group of the organic linker of the MOF [35]. The vibrational modes of amino group overlap with that of the O-H bands of the carboxylic group and broad peak of H_2O.

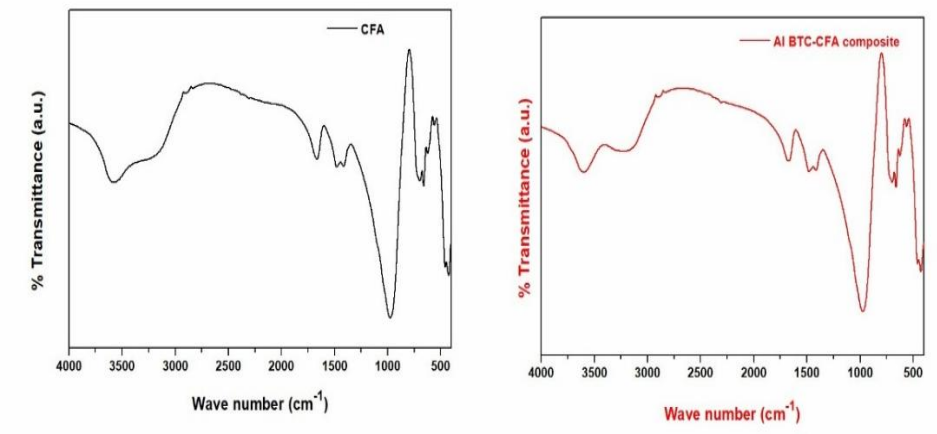

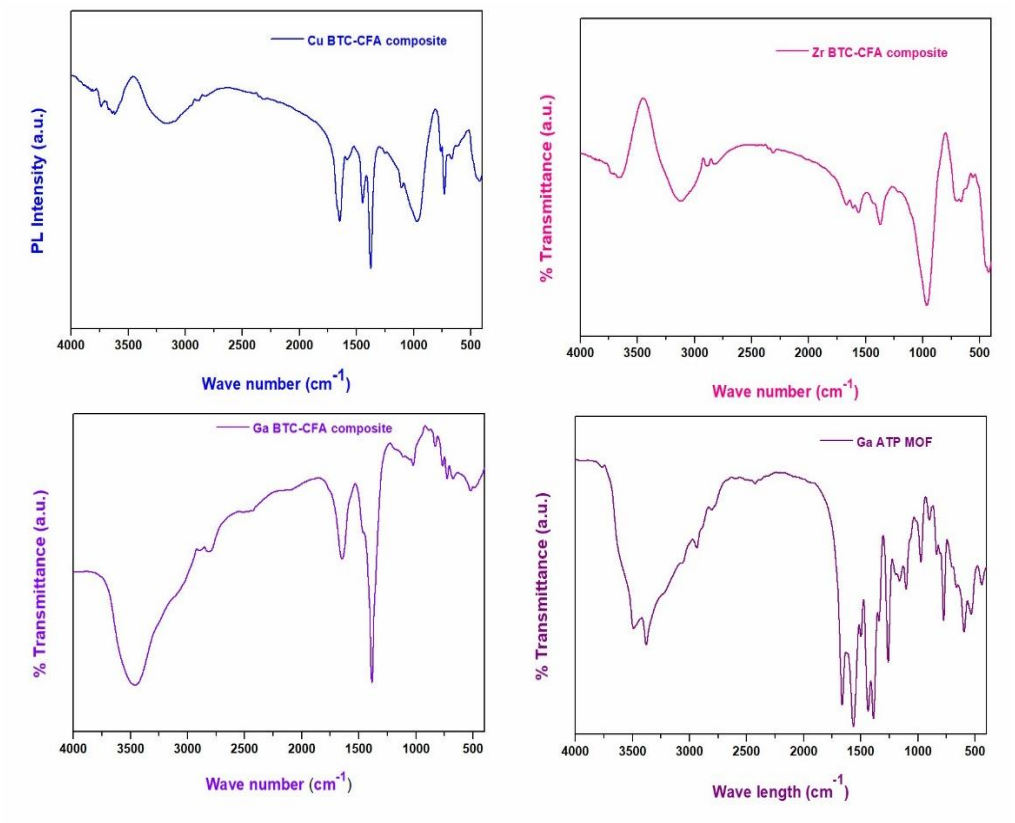

Figure 5: FT-IR spectra of MOF-CFA composites and Ga-ATP MOF

Raman Spectral Analysis

Raman spectra (fig. 6) were not very specific for the MOF-CFA composites as only intense vibrational mode is observed as a broad band in between 0-500 cm^{-1} and very low intense peaks were observed at 1450 and 1629 cm^{-1} probably due to N-H vibrational modes in Ga-ATP MOF [36]. The broad peak observed indicate the M-O-M modes of MOFs in the composites [32]. Most of the MOF characteristic peaks were masked due to the dominant composition of CFA material in the composites.

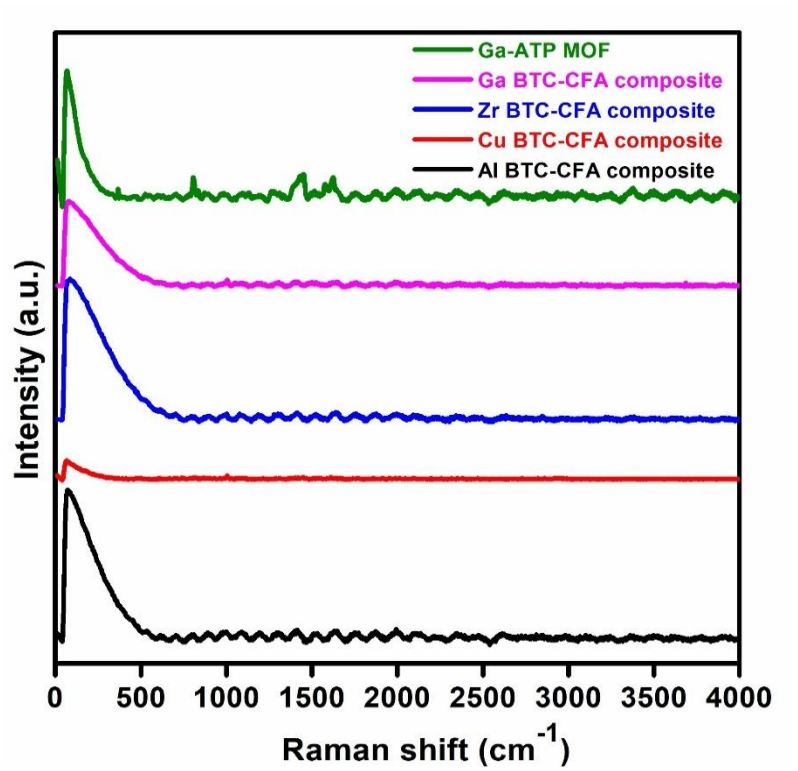

Figure 6: Raman spectra of MOF-CFA composites & Ga-ATP MOF

UV-DRS Spectra

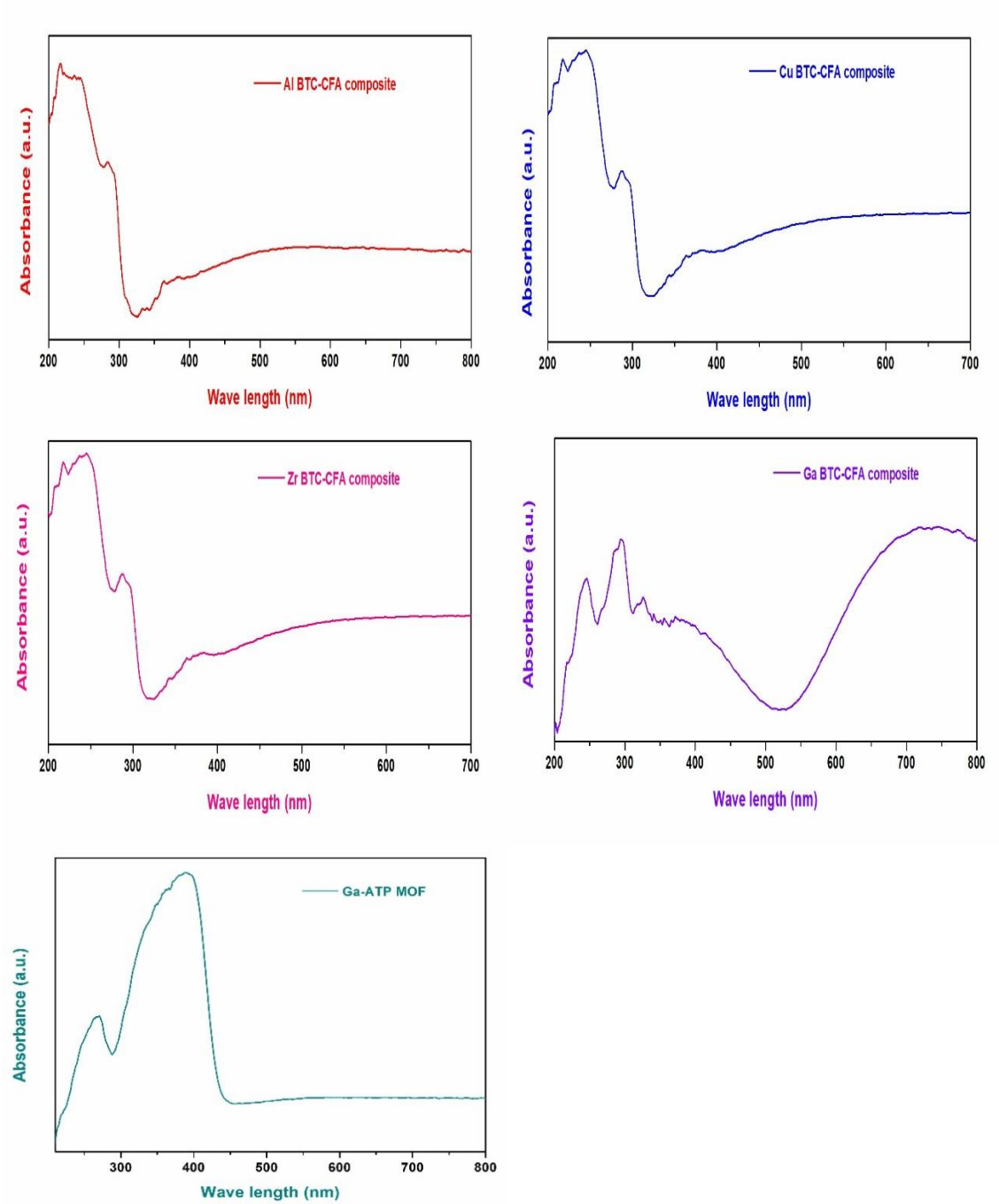

Figure 7: UV-DR spectra of BTC MOF-CFA composites and Ga-ATP MOF

The absorption of all the BTC MOF-CFA composites of Al, Zr and Cu were observed in the range of 200-300 nm while that of Ga BTC MOF-CFA composite extended upto 500 nm (fig. 7). The presence of CFA has a blue shift in the absorption towards lower wave length in case of Cu BTC composite and Al BTC composite which exhibited lower absorption wave lengths than their pristine forms [32]. While Ga BTC composite retained the absorption upto 500 nm even in presence of CFA. Ga-ATP MOF absorption was in the range of 200-450 nm lower than Ga BTC MOF. The same was reflected in its Tauc plot (figure 8) which showed a band gap = 2.84 eV higher than Ga BTC MOF (E_g = 2.2 eV) [32]. The band gap energies of Cu BTC and Al BTC MOF composites were also higher as compared to their pure MOFs owing to the lower absorption wave lengths since CFA is the dominant component in the composites. Zr BTC MOF composite showed high band gap (3.74 eV) as well closer to that of Al BTC MOF composite (3.9 eV). It is in line with absorption of these composites mainly in UV region.

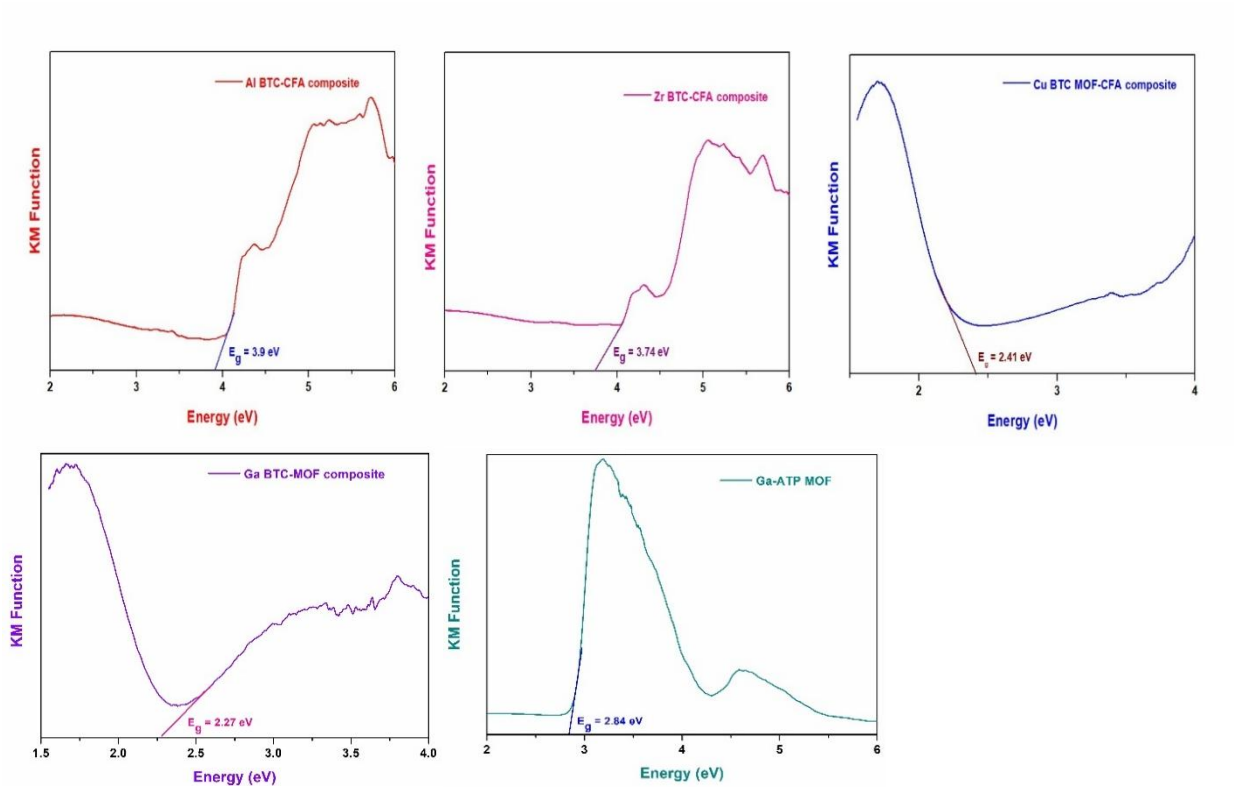

Figure 8: Tauc Plots of BTC MOF-CFA composites and Ga-ATP MOF

XPS Analysis

The surface analysis of the four different MOF-CFA composites was done by XPS and their corresponding spectra of the various elements of the respective composites as well as that of Ga-ATP MOF are presented in figure 9. Al 2p spectrum was obtained at a B.E. of 73.6 eV, Zr $3d_{5/2}$ and $3d_{3/2}$ can be seen at 182.2 and 184.5 eV respectively and Cu $2p_{3/2}$ and $2p_{1/2}$ are observed at 933 and 953 eV respectively with a presence of very weak satellite peaks just beside them. Ga^{3+} presence can be observed from its XPS spectra of Ga $2p_{1/2}$ at 1119 and 1190.2 eV and, Ga $2p_{3/2}$ at 1110 and 1110.2 eV in case of Ga-ATP MOF and Ga BTC MOF-CFA composite respectively. The B.E. of Ga 2p is slightly at a higher energy in case of the Ga MOF composite as compared to Ga-ATP MOF. The common elements in all these samples are C, O and N. C1s could be seen at a B.E. of 284.7 eV in case of Ga-ATP MOF and at 284.5 eV in case of the MOF composites. A should peak is observed around 288.5 and 288.7 eV respectively with the ATP MOF and composite of Ga. The former corresponds to aromatic carbon in the terephthalic acid organic linkers while the latter at around 288.7 eV is due to the carboxylic acid group [37]. O1s B.E. shifted from 531.3 eV to 532 eV in case of MOF-CFA composites of Al, Zr, Cu and Ga with a difference of 0.2 eV from Al to Ga as can be observed from the fig. 9 below. N1s peak is very weak and negligible intensity in case of composites as it is probably due to the presence of the small amounts of solvent N,N-DMF while Ga-ATP indicated an intense peak at around 399.3 eV owing to the presence of amino group. Na1s is present in all the MOF-CFA composites owing to the Na modification carried out for coal fly ash material to enhance its absorption capacity of heavy metal ions.

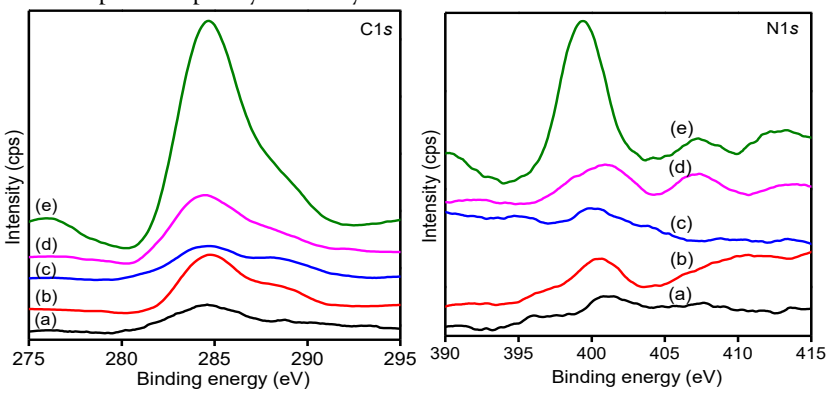

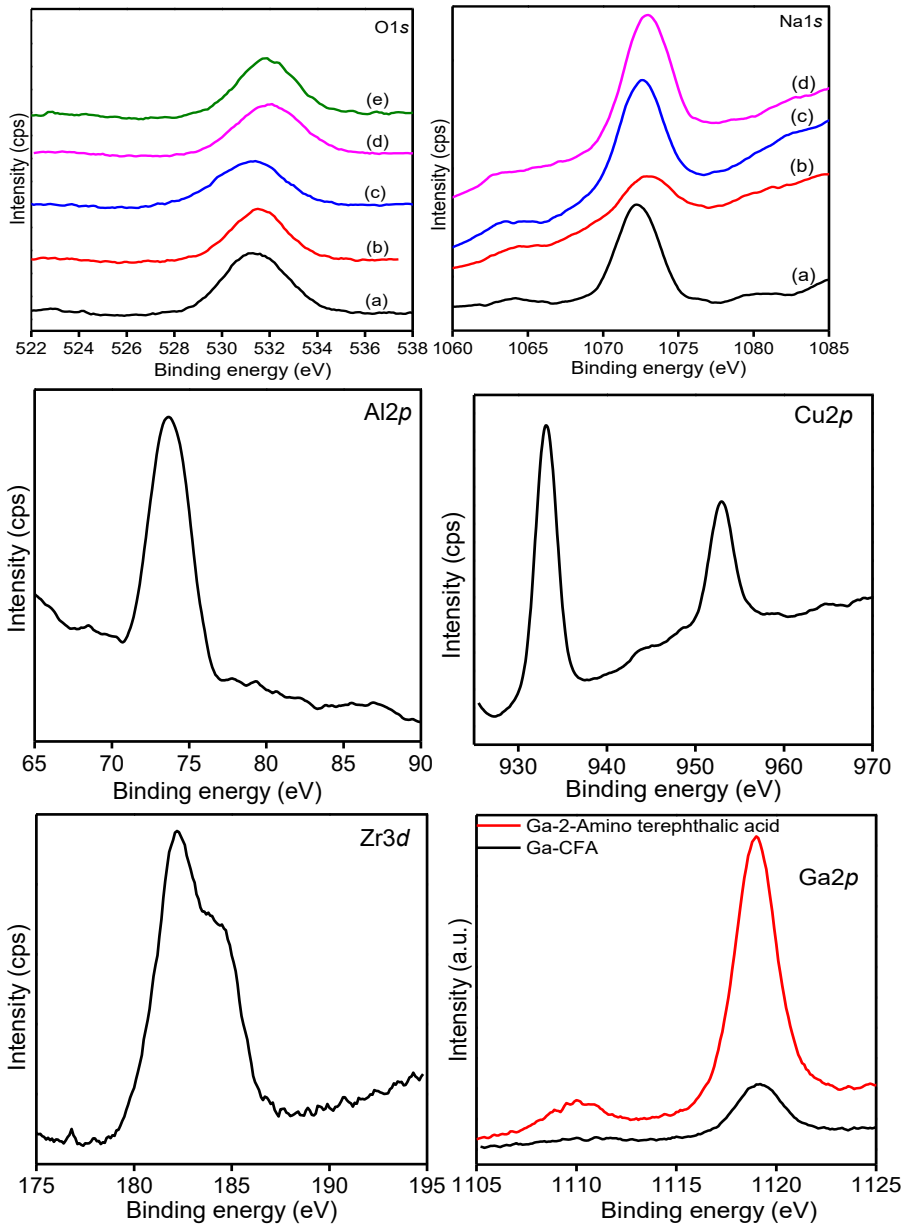

Figure 9: XPS of (a) Al BTC-CFA, (b) Cu BTC-CFA, (c) Zr BTC-CFA, (d) Ga BTC-CFA and (e) Ga BTC-ATP

Toxic heavy metal ion removal by MOF-CFA composites

Our previous studies on BTC based MOFs showed that these materials possessed high potential for the adsorption of heavy metal ions. Among the four, the adsorption efficiency of Ga BTC MOF much higher and to increase its removal efficiency the organic linker viz., amino terephthalic acid was used in place of benzene tricarboxylic acid as the presence of amine group is known to enhance the selective adsorption of heavy metal ions through chelation [34]. Also, to further enhance their adsorption capacity and with the aim to utilize coal fly ash, a low cost and abundantly available material, the four different BTC MOFs studied were combined in-situ with sodium modified coal fly ash to obtain the composites. All these five materials were explored for the adsorption of Pb(II), Hg(II) and Cd(II) ions from their respective aqueous solutions taken in a batch mode. A definite amount of about 50 mL of the heavy metal ion aq. solution was taken each time with about 10 mg of the adsorbent stirred at ambient temperature, centrifuged to separate the adsorbent and the metal ion solution. Samples were collected at different intervals of time. The solution after adsorption was tested for the remaining concentration of the heavy metal ion by ICPOES analysis while the adsorbent separated by centrifugation was analyzed by SEM-EDX analysis. Different sets of experiments were carried out in order to understand the effect of pH, amount of adsorbent, concentration of the metal ions etc., to optimize the conditions to achieve maximum possible removal efficiency of the metal ions over the composites in this study.

Effect of pH on the removal efficiency of Ga BTC-MOF composite

The previous studies using pristine MOFs for the heavy metal ion removal indicated a pH of 6 to be optimum in the study. However, since the MOFs are combined with Na modified CFA, the CFA material is known to show higher efficiency in the metal ion adsorption at higher pH conditions, hence, the metal ion adsorption was tested at variable pH from 1-10 over Ga BTC-MOF composite. 200 ppm of the three heavy metal ions solutions were studied at varying pH. The figure 10 below shows that the adsorption capacity of the composite raised with pH and it was maximum at 8 and remained the same till pH 10 and later further increase in pH resulted in the reduction of the adsorption efficiency of the composite. Hence a pH of 8 was maintained through this study.

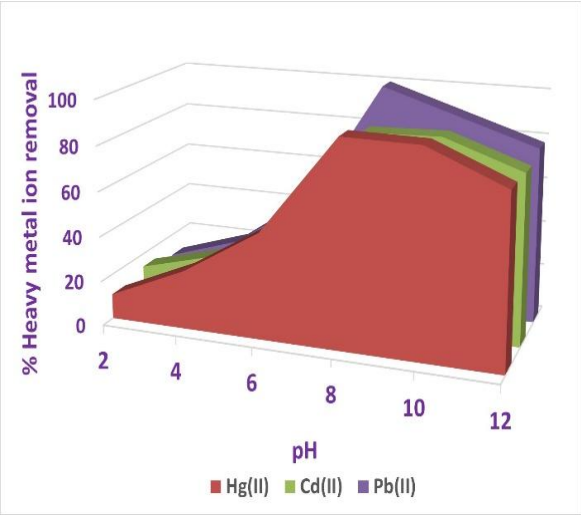

Figure 10: Heavy metal ion removal vs pH over Ga-CFA composite

Influence of MOF: CFA composition on the removal efficiency of Pb (II) over Ga BTC MOF-CFA composite

Composites of four different compositions of MOF: CFA i.e., 0.1-0.9, 0.2-0.8, 0.3-0.7 and 0.4-0.6 were prepared and studied for the removal of Pb (II) ions over Ga BTC MOF-CFA composite at ambient conditions using 400 ppm of Pb (II) solution. The removal efficiency of these composites was compared with that of their pure components viz., CFA and Ga BTC MOF. The table 2 given below shows the data of this study from which it may be deduced that the MOF: CFA composition of 0.3-0.7 is optimum to achieve best results in terms of the removal of the heavy metal ions.

Table 2: Pb(II) removal efficiency over Ga BTC MOF-CFA composites of variable MOF-CFA compositions

Ga BTC MOF-CFA Composition	% Pb (II) Adsorption
0-1	55
0.1-0.9	69
0.2-0.8	85
0.3-0.7	100
0.4-0.6	90
1-0	49

Variation of heavy metal ion removal efficiency over MOF-CFA composites & Ga-ATP MOF (Effect of nature of adsorbent)

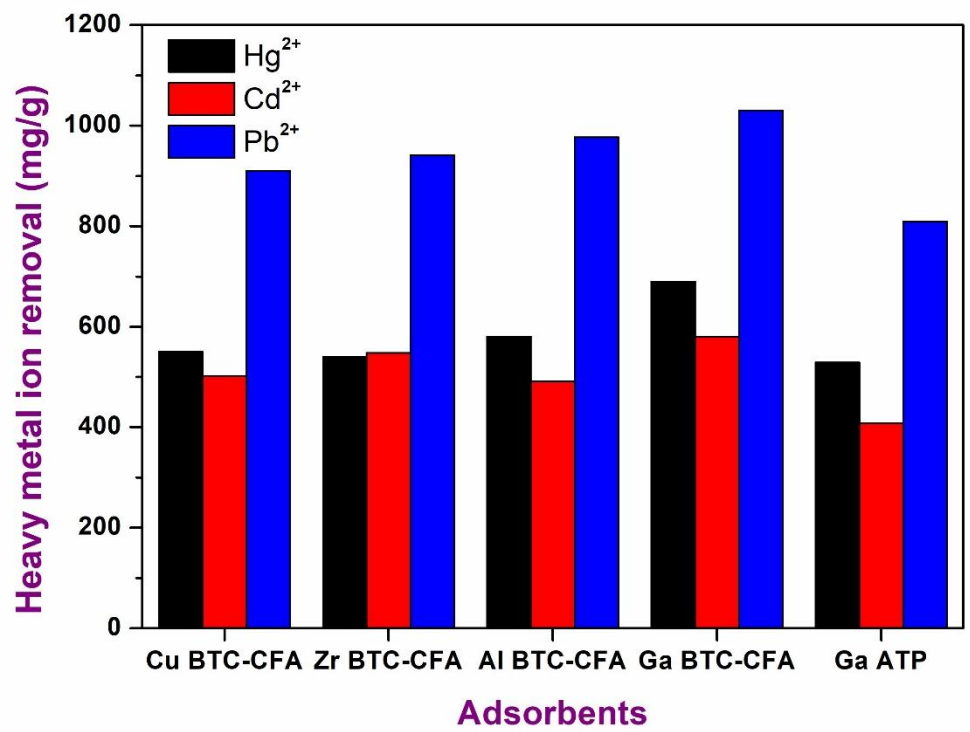

Figure 11: Variation of heavy metal ion removal efficiency with adsorbent

200 ppm at pH 8 and ambient temperature, the adsorption efficiency of Pb(II), Hg(II) and Cd(II) removal from their respective aqueous solutions was studied over all the four different MOF-CFA composites and Ga-ATP MOF. This study that is depicted in the figure 11 clearly indicates that the % removal of Pb(II) >> Hg(II) > Cd(II) over all the adsorbents studied. Among the three ions, the adsorbents were found to be more selective in the removal of Pb(II). The removal efficiency of Pb(II) over the adsorbents is found to be in the order Ga BTC-CFA > Al BTC-CFA > Ga-ATP MOF > Zr BTC-CFA > Cu BTC-CFA.

Effect of contact time over Ga BTC-CFA composite in the removal of heavy metal ions

Figure 12 represents the change in the adsorption efficiency of heavy metal ions over Ga BTC-CFA composite with time. The initial concentration of Pb(II) taken was 400 ppm while those of Hg(II) and Cd(II) taken were of 200 ppm concentration. A maximum adsorption of the three ions was achieved with in 30 min. of adsorption and a constant adsorption was observed till 5 h (300 min.). The composite material is found to be more effective as the maximum adsorption could be obtained within 30 min. while over pristine Ga BTC MOF the same was achieved after 60 min. of time. A maximum of 1983 mg/g of Pb(II) removal was evidenced over Ga BTC-CFA composite while 690 and 580 mg/g of Hg(II) and Cd(II) removal is attained on the same composite within 30 min. of adsorption.

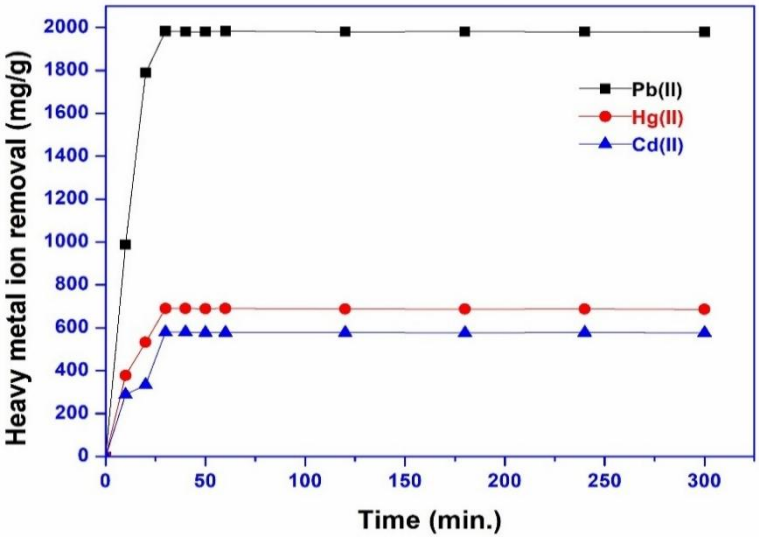

Figure 12: Effect of contact time on the adsorption of heavy metal ions over Ga BTC MOF-CFA composite

Adsorption Kinetics

Effect of initial concentration on the Pb(II) removal efficiency of Ga BTC MOF-CFA composite

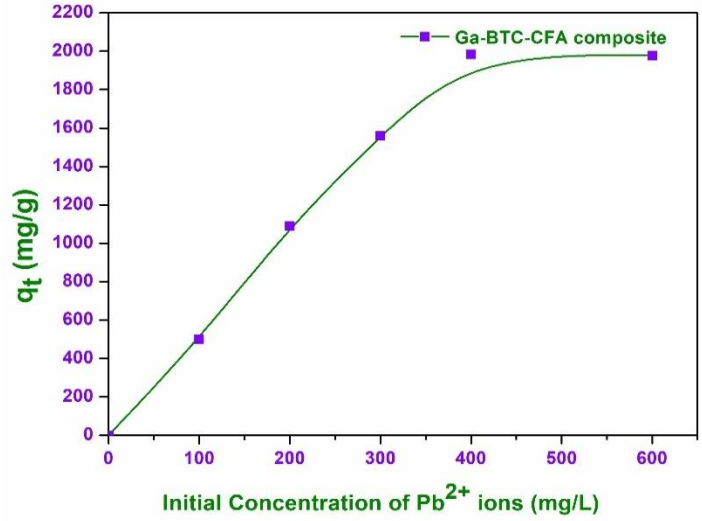

Figure 13: Pb (II) removal efficiency vs initial concentration of Pb (II) over Ga BTC MOF-CFA composite

Our previous report showed that the adsorption of heavy metal ions over MOFs follows a pseudo II-order kinetics and the below model equation was found to be the right fit for the experimental data obtained.

$$\frac{t}{q_t} = \frac{1}{k_2 q_e^2} + \frac{1}{q_e} t$$

where q_e = amount of heavy metal ions adsorbed at equilibrium in (mg g^{-1});
q_t = amount heavy metal ions adsorbed at any time t in (mg g^{-1}); t = time in min.; and
k_2 = pseudo second order rate constant (g $mg^{-1}min^{-1}$).

Effect of initial concentration on the removal efficiency of Pb(II) was studied on Ga BTC MOF-CFA composite (fig.13) which was best among the rest of the adsorbents in this work. The concentration of aqueous solution of Pb(II) increased from 100 ppm to 600 ppm. This composite had adsorbed almost 100% of the lead ions (1983 mg/g) upto 400 ppm and later a saturation of the adsorption capacity was noticed at 600 ppm exhibiting the same q_t value.

The present data of adsorption kinetics followed in the removal of Pb(II), Hg(II) and Cd(II) over Ga BTC MOF-CFA composite showed a good fit into the pseudo second order equation mentioned above. The figure 14 shows the linear fit of the data and their corresponding rate constants and R^2 values are presented in table 3. The high R^2 values indicate the proper linear fit of the adsorption kinetics data into the chosen model.

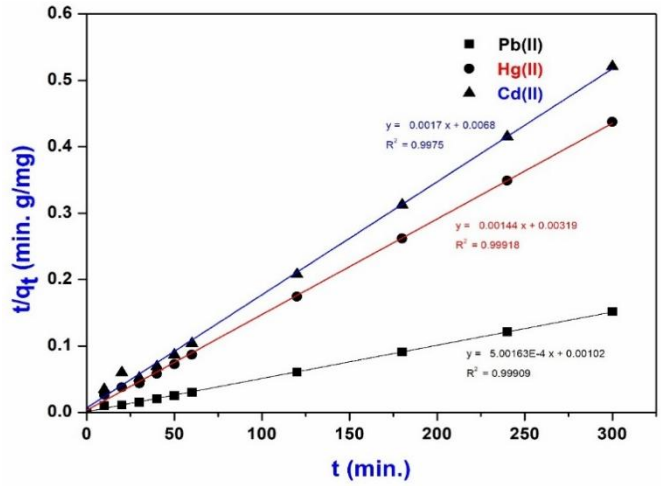

Figure 14: Kinetic plot of adsorption of heavy metal ions over Ga BTC MOF-CFA composite, t/q_t vs t

Table 3: Pseudo II order kinetics characteristics of heavy metal ion adsorption over Ga BTC MOF-CFA composite

Heavy metal ion	k_2 x 10^4 ($g \cdot mg^{-1} \cdot min^{-1}$)	R^2 (Correlation coefficient)
Pb(II)	2.54	0.99909
Hg(II)	6.50	0.99919
Cd(II)	4.25	0.99750

Reusability and stability of the Ga MOF-CFA composite

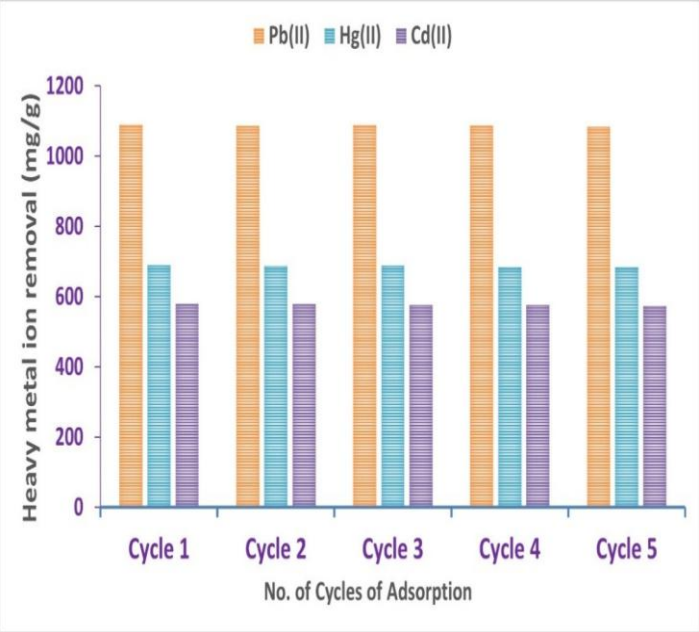

Figure 15: Reusability of Ga BTC MOF-CFA for the adsorption of heavy metal ions

The reusability of the Ga MOF-CFA composite showed that it can be recycled after each adsorption run and washing with DMF/water followed by drying in oven at 80 °C for at least 5 cycles. The adsorbent was found to be structurally intact and stable after these 5 cycles as can be seen from its XRD and SEM images in the figure 16 below.

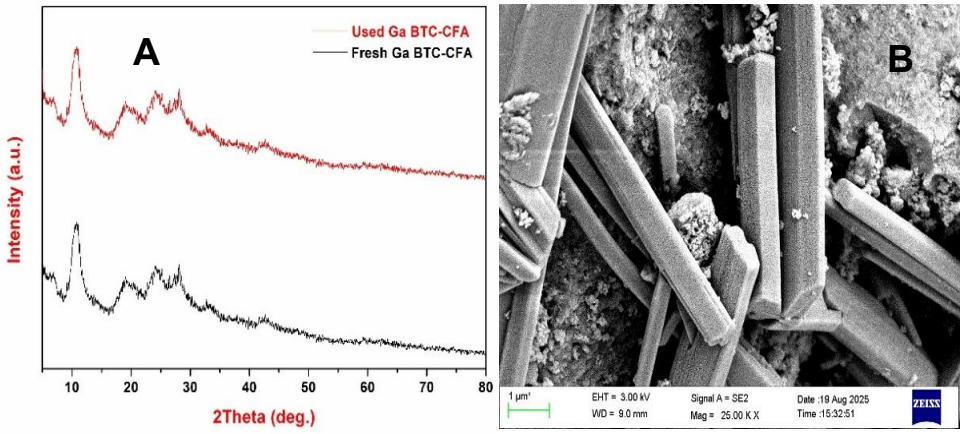

Figure 16: A). XRD patterns of Fresh and used Ga BTC MOF-CFA composite
B). SEM micrograph of used Ga BTC MOF-CFA composite

The presence of adsorbed Pb (II), Hg (II) and Cd (II) ions over Ga BTC MOF-CFA composite is confirmed from the SEM-EDX and elemental mapping done on the used composite after adsorption for 5 h using 200 ppm of the heavy metal ion solutions.

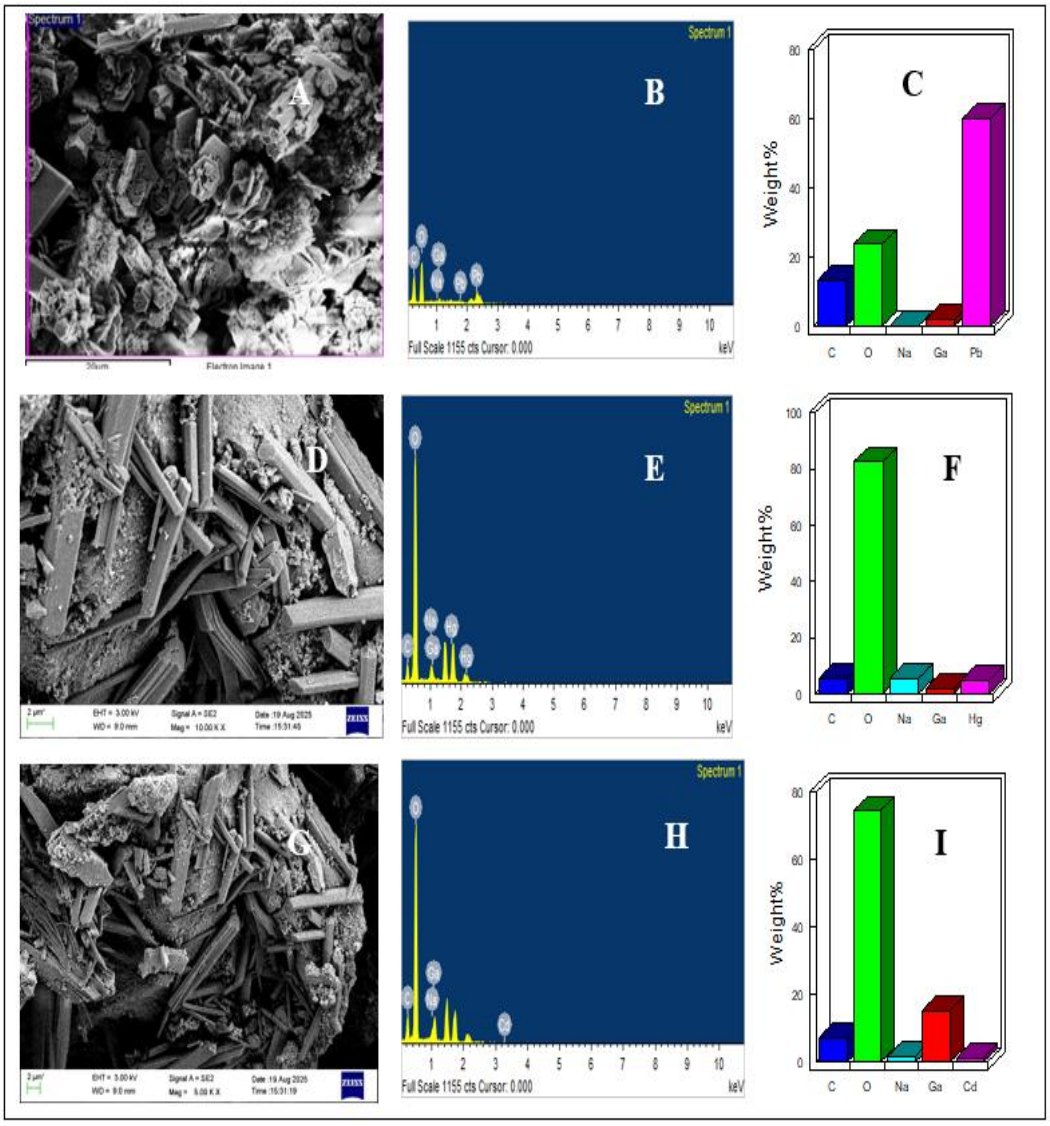

Figure 17: SEM-EDX & Elemental composition of adsorption of Pb (II)-A), B) & C); Hg (II)- D), E) & F);
Cd (II)-G), H) & I)) over Ga-BTC MOF-CFA composite

CONCLUSIONS

MOF-CFA composites were synthesized by solvo-hydrothermal technique combining CFA in-situ in the MOF synthesis. The composites were well characterized and found that all the composites were though having smaller but micro- crystallites with changes in morphology and reduction in surface characteristics such as surface area and porosity. The Ga-ATP MOF showed all the specific features of a MOF material. These samples showed much enhanced adsorption efficiency in the removal of Pb (II), Hg (II) and Cd (II) ions from water as compared to their pristine MOFs. The % removal of Pb (II) >> Hg (II) > Cd (II) over all the adsorbents studied. Ga-ATP MOF also exhibited higher removal efficiency as against the Ga-BTC MOF. The removal efficiency of Pb (II) over the adsorbents is found to be in the order Ga BTC-CFA > Al BTC-CFA > Ga-ATP MOF > Zr BTC-CFA > Cu BTC-CFA. Among all the four different MOF composites Ga BTC-CFA higher efficiency in the removal of heavy metal ions. And its removal efficiency towards Pb (II) was found to be highest of about 1983 mg/g. The removal efficiency was also improved in terms of higher rate of removal as compared to the pristine Ga-BTC MOF (k_2 = 3.125 x 10^{-2}). Ga BTC-CFA is found to be stable and reusable up to at least 5 cycles for the removal of heavy metal ions. Thus, addition of a cheap and waste material CFA to MOF generated a composite of better adsorption efficiency in the removal of heavy metal ions.

CONFLICT OF INTEREST

Authors declare no conflict of interest.

ACKNOWLEDGEMENTS

The authors are grateful to Central Facility for Research & Development, Osmania University, Hyderabad for the XPS analysis, to the Department of Chemistry, Osmania University for the XRD and FT-IR analyses and to Dr. A. Venugopal, Chief Scientist, CSIR-IICT, Hyderabad for some of the characterization of the samples in this study.

REFERENCES

[1] Yaghi, O.M.; O'Keeffe, M.; Ockwig, N.W.; Chae, H.K.; Eddaoudi, M.; Kim, J. Reticular synthesis and the design of new materials. Nature 2003, 423, 705–714.
[2] Lee, J.; Farha, O.K.; Roberts, J.; Scheidt, K.A.; Nguyen, S.T.; Hupp, J.T. Metal-organic framework materials as catalysts. Chem. Soc. Rev. 2009, 38, 1450–1459.
[3] Mueller, U.; Schubert, M.; Teich, F.; Puetter, H.; Schierle-Arndt, K.; Pastré, J. Metal-organic frameworks—Prospective industrial applications. J. Mater. Chem. 2006, 16, 626–636.
[4] Beurroies, I.; Boulhout, M.; Llewellyn, P.L.; Kuchta, B.; Férey, G.; Serre, C.; Denoyel, R. Using pressure to provoke the structural transition of metal-organic frameworks. Angew. Chem. Int. Ed. 2010, 49, 7526–7529.
[5] Xiao, J.; Wu, Y.; Li, M.; Liu, B.-Y.; Huang, X.-C.; Li, D. Crystalline structural intermediates of a breathing metal-organic framework that functions as a luminescent sensor and gas reservior. Chem. Eur. J. 2013, 19, 1891–1895.
[6] Khan, N.A.; Hasan, Z.; Jhung, S.H. Adsorptive removal of hazardous materials using metal-organic frameworks (MOFs): A review. J. Hazard. Mater. 2013, 244–245, 444–456.
[7] Li, J.-R.; Sculley, J.; Zhou, H.-C. Metal-organic frameworks for separations. Chem. Rev. 2012, 112, 869–912.
[8] Maspoch, D.; Ruiz-Molina, D.; Wurst, K.; Domingo, N.; Cavallini, M.; Biscarini, F.; Tejada, J.; Rovira, C.; Veciana, J. A nanoporous molecular magnet with reversible solvent-induced mechanical and magnetic properties. Nat. Mater. 2003, 2, 190–195.
[9] Sudik A C, Antek P C, Foy G W, O'Keeffe M and Yaghi O M, A metal-organic framework with a hierarchical system of pores and tetrahedral building blocks, 2006, Angew. Chem Int Ed Engl, 45, 2528-2533.
[10]Chen B L, Ockwig N W, Millard A R, Contreras D S and Yaghi O M, High H2 adsorption in a microporous metal-organic framework with open metal sites, 2005, Angew Chem Int Ed Engl, 44, 4745-4749.
[11]Kim J, Lin B, Reineke T M, Li H, Eddaoudi M, O'Keeffe M and Yaghi O M, Rod packings and metal-organic frameworks constructed from rod-shaped secondary building units, 2001, J Am Chem Soc, 123, 8239-8247.
[12]Rowsell, J. L. C.; Yaghi, O. M, Metal–organic frameworks: a new class of porous materials, Micropor. Mesopor. Mater., 2004, 73, 3-14.
[13]Barakat M A, New Trends in Removing Heavy Metals from Industrial Wastewater, 2011, Arab J Chemistry, 4, 361-377.
[14]Kobielska P A, Howarth A J, Farha OK, Nayak S, Metal–organic frameworks for heavy metal removal from water, 2018, Coord Chem Rev 358, 92-107.
[15]Hatzidaki E, Tzanakakis G N and Tsatsakis A M, Lead toxicity update. A brief review, 2005, Med Sci Monit, 11(10), 329–336.
[16]Karababa H, Atasoy M, Yildiz D, Kula I and Tuzen M, Development of a Sensitive Method for Cadmium Determination in Fish Tissue and Drinking Water Samples by FAAS Using SQT In Situ Atom Trapping, 2023, ACS Omega, 8, 7063–7069.
[17]Ledezma C Z-, Bolagay D N-, Figueroa F, Ledezma E Z-, Ni M, Alexis F and Guerrero V H, Heavy metal water pollution: A fresh look about hazards, novel and conventional remediation methods, 2021, Environ Technol Innovation, 22, 101504.
[18]Imran Ali, New Generation Adsorbents for Water Treatment, 2012, Chemical Reviews 112 (10), 5073-5091.
[19]Xu S, Lv Y, Zeng X, Cao D, ZIF-derived nitrogen-doped porous carbons as highly efficient adsorbents for removal of organic compounds from wastewater, 2017, Chem Eng J, 323, 502–511.
[20]Sublet R, Simonnot M -O, Boireau A, Sardin M, Selection of an adsorbent for lead removal from drinking water by a point-of-use treatment device, 2003, Water Res 37(20), 4904–4912.
[21]Edokpayi JN, Odiyo JO, Popoola EO, Alayande OS, Msagati TAM, Synthesis and Characterization of Biopolymeric Chitosan Derived from Land Snail Shells and Its Potential for Pb2+ Removal from Aqueous Solution. 2015, Materials (Basel). 10;8(12):8630-8640.
[22]C. G. Jun, K. Y. Sam, and J. C. Nag, "Application of fly ash as an adsorbent for removal of air and water pollutants," 2018, Applied Sciences, 8(7), p. 1116.
[23]V. P. Suhas, C. N. Suryakant, and J. K. Sunil, "Industrial applications of fly ash: a Review," 2013, International Journal of Science, Engineering and Technology Research, 2 (9), 1659-1663.
[24]Ishwari B.K 1, Kumar P.S, Shivaprasad K.H, Adsorption Studies of Heavy Metals on Coal Fly Ash Samples from Aqueous Solutions, 2022, Applied Ecology and Environmental Sciences, 10 (1), 25-33.
[25]Abd El Salam, H. M., & Zaki T, A Novel Microwave Synthesis of Manganese Based MOF for Adsorptive of Cd(II), Pb(II) and Hg(II) Ions from Aqua Medium. 2019, Egyptian Journal of Chemistry, 62(5), 837–851.
[26]Chena, S., Fenga, F., Lia, S., Lia, X.-X., & Shu, L. Metal-organic framework DUT-67 (Zr) for adsorptive removal of trace Hg2+ and CH3Hg+ in water. 2018, Chemical Speciation and Bioavailability, 30(1), 99–106.
[27]Saleem H, Rafique U and Davies R P, Investigations on post-synthetically modified UiO-66-NH2 for the adsorptive removal of heavy metal ions from aqueous solution, 2016, Microporous and Mesoporous Materials, 221, 238-244.
[28]Huang Z, Zhao M, Wang C, Wang S, Dai L, Zhang L, Preparation of a Novel Zn(II)-Imidazole Framework as an Efficient and Regenerative Adsorbent for Pb, Hg, and As Ion Removal From Water, 2020, ACS Appl Mater Interfaces, 12, 41294–41302.

[29]Ke F, Qiu L G, Yuan Y P, Peng F M, Jiang X, Xie A J, Shen Y H and Zhu J F, Thiol-functionalization of metal-organic framework by a facile coordination-based post synthetic strategy and enhanced removal of Hg2+ from water, 2011, J Hazard Mater, 196, 36-43.
[30]Bakhtiari, N., & Azizia, S, Adsorption of copper ion from aqueous solution by nanoporous MOF-5: a kinetic and equilibrium study, 2015, J. Mol. Liq., 206, 114-118.
[31]Boix, G., Troyano, J., Tovar, L. C. G., Camur, C., Bermejo, N., Yazdi, A., Piella, J., Bastús, N. G., Puntes, V., Imaz, I., & Maspoch, D. MOF-Beads containing inorganic nanoparticles for the simultaneous removal of multiple heavy metals from water. 2020, ACS Applied Materials & Interfaces, 12(9), 10554–10562.
[32]Swaroopa Ch, Vennela A, Venkatesham K, Vijayalaxmi B, Vijayatha M, Venkataswamy P, Sasikumar B, Anjaneyulu C, Ramaswamy K, Hari Padmasri A, M-BTC (M = Ga, Zr, Al, Cu) MOFs For The Efficient Removal Of Toxic Heavy Metal Ions From Water: Synthesis, Characterization And Adsorption Studies, 2025, International Journal of Environmental Sciences, 11 (21s) 4357-4379.
[33]Aniruddha, R., Singh, S.A., Reddy, B.M., Venugopal, A., Sreedhar, I., Coal fly ash - ZIF-8 composites for enhanced and stable carbon capture—An in-depth study. 2024, Mater. Adv. 5, 8709–8729.
[34]Awad S F, Bakry A M, Ibrahim A A, Lin A & El-Shall M S, Thiol-and amine-incorporated UIO-66-NH2 as an efficient adsorbent for the removal of Mercury (II) and phosphate ions from aqueous solutions, 2021, Ind Eng Chem Res 60, 12675–12688.
[35]Wu, L.; Qin, D.; Fang, F.; Wang, W.; Zhao, W. Development of Efficient Photocatalyst MIL-68(Ga)_NH2 Metal-Organic Framework for the Removal of Cr(VI) and Cr(VI)/RhB from Wastewater under Visible Light, 2022, Materials 15, 3761.
[36]Karthik, P., Vinoth, R., Zhang, P., Choi, W., Balaraman, E., and Neppolian, B., π–π Interaction between metal-organic framework and reduced graphene oxide for visible-light photocatalytic H2 production, 2018, ACS Appl. Energy Mater., 1 (5), 1913–1923.
[37]J. Cheng, X. Xuan, X. Yang, J. Zhou and K. Cen, Preparation of a Cu(BTC)-rGO catalyst loaded on a Pt deposited Cu foam cathode to reduce CO2 in a photoelectrochemical cell, RSC Adv., 2018,8, 32296-32303.